

Operational Behavior of Graded Diamond Grinding Wheels For End Mill Cutter Machining

Berend Denkena

Leibniz Universität Hannover

Benjamin Bergmann

Leibniz Universität Hannover

Daniel Raffalt (✉ raffalt@ifw.uni-hannover.de)

Institut für Fertigungstechnik und Werkzeugmaschinen

Research Article

Keywords: deep grinding, graded grinding tools, simulation-based grinding wheel design, hybrid-bond grinding wheels

Posted Date: November 3rd, 2021

DOI: <https://doi.org/10.21203/rs.3.rs-973250/v1>

License: © ⓘ This work is licensed under a Creative Commons Attribution 4.0 International License.

[Read Full License](#)

Abstract

The varying related material removal rate during deep grinding of cemented carbide end mill cutters results in an unevenly wear of the grinding wheel. This causes a reduced geometrical precision of the manufactured tools. Consequently, the intervals between dressing steps are reduced and the dressing infeed increases. The aim of this research project is therefore to design a tailored grinding tool with uniform wear behavior. To address this situation, the grinding tool load is determined simulatively along the width of the grinding wheel. From this an equation is derived to adapt the bonding layer properties to the local load differences. First investigations show that two different concentrations zones in the abrasive layer of the grinding wheel improves the wear behavior already. This indicates that a further reduction of the wear difference is possible by a more uniform gradient. A simulation is performed to define a knowledge based gradient with more than two concentration zones. This allows a more precise load optimized adaptation of the grinding layer properties to the geometry to be ground in terms of wear behavior. Grinding tools manufactured on this basis are used for flute grinding of end mill cutters. A reduction of the wear difference over the grinding wheel width of 52% and an improved cutting edge quality of these are demonstrated.

1) Introduction

The properties of cemented carbides, such as high hardness, wear resistance and low ductility, lead to a high wear during grinding. Therefore, highly wear-resistant diamond grinding wheels are used for the processing of these materials [1, 2]. In flute grinding in particular, a very high related material removal rate occurs which, due to the strongly varying geometric engagement conditions, simultaneously varies significantly over the width of the grinding tool. [3, 4] This results in local deviations in the wear behavior of the grinding wheel and thus, the grinding precision decreases with increasing wear. To prevent this, the time between dressing steps must be reduced to guarantee the targeted precision of the grinding process. *Schröer* shows in his work that a grinding wheel with two different concentration zones, C150 and C100, reduces the differences in the wear behavior already to a certain amount [5]. A finer graduation of the grinding wheel properties than only in two zones would be useful for leveling the wear behavior. Another possibility for the load adjustment over the grinding wheel width is the grain size. Smaller grains reduce the forces per grain [6] and enhance the tool surface quality [7]. Therefore the grinding wheels exhibit a hybrid bond. The use of hybrid bond grinding wheels with a combination of a resin and a metallic bond allows the combination of high productivity and high surface qualities [8, 9]. A cutting edge with less defects is important for the operational behavior of the end mill cutters [3, 10]. This paper presents a knowledge-based model for reducing wear differences in flute grinding. Furthermore, an experimental validation of the model by analyzing the result of deep grinding of end mill cutters with grinding wheels based on the model is presented. For this purpose, two non graded grinding wheels are compared with three graded grinding wheels. As gradients a concentration gradient and two gradients with the variation of grain size and the concentration are investigated.

2) Materials And Methods

2.1 Simulative approach

A model for calculating a gradient is developed. The model achieves wear leveling by adapting the area-related number of grains to the local related material removal rate. This requires knowledge of the course of the related metal removal rate over the grinding tool width. An increase in the local related material removal rate also means a local increase in load during grinding. The local related material removal rate depends on the depth of cut a_e and the feed rate v_f , as described in equation 1, and thus enables a statement to be made about the local mechanical and thermal load on the grinding tool [11, 12].

$$Q'_w = a_e \cdot v_f (1)$$

For the determination of Q'_w the technological NC-based material removal simulation IFW CutS was used [13]. The simulation is Dixel-based and the material removal on the workpiece is represented by the three Boolean operations shorten, divide and remove dexels. In the simulation the tool grinding machine Walter Vision Helitronic, the grinding tool and the workpiece are implemented. By using the HELITRONIC TOOL STUDIO software to generate NC-Codes the kinematics are obtained. In this study, the model is set up and validated using a cutter geometry with a diameter of d_s of 16 mm, and a helix angle δ of 30°. The depth of cut is varied. This results in different core diameters with the core diameter factors k of 0.8, 0.7, 0.6 and 0.5. To consider the influence of the feed rate on Q'_w , it is varied in the simulation in two steps from 150 mm/min to 300 mm/min. From this simulation, a formula is derived in chapter 3 for creating gradients based on the adjustment of the area-related number of grains.

2.2 Experimental setup

All grinding wheels for flute grinding have a 1A1 geometry with a diameter of 100 mm and a width of 10 mm. Based on the results of the simulation, three graded grinding wheels, were produced by the grinding tool manufacturer Dr. Müller Diamantmetall AG. Two grinding wheels with constant abrasive layer properties are used in the following investigations as a reference to the graded grinding wheels, with different grain concentration and grain size. The first one with a grain concentration of C100 (in vol. %) and a grain size d_g of 46 μm and the second with a concentration of C125 and a grain size of 54 μm . The bond material for flute grinding is a hybrid bond of resin and metal. These grinding wheels were used for the flute grinding of ten cemented carbide end mill cutters each. The specification EMT210 by the company Extramet was used as carbide blanks. (Grain size: 0.8 μm Co content: 10 wt. %). The process was performed on a tool grinding machine Vollmer VHybrid360. The geometrical specifications of the end mills are a helix angle δ of 30°, a flute length l_c of 45 mm, an end mill cutter diameter of 16 mm, a core diameter d_k of 11.2 mm and a number of teeth z of four. A cutting speed v_c of 18 m/s and a feed rate v_f of 180 mm/min were used as process parameters. To analyze the cutting edges of the milling tool, it is necessary to grind the flank faces and the end faces. The end face processing was done by a 12V9 resin bond diamond grinding wheel with a v_c of 25 m/s and a v_f of 50 mm/min. Grain size and

concentration of this grinding wheel are D64 and C100. The flank face processing was done by an 11V9 grinding wheel, with a v_c of 25 m/s and a v_f of 70 mm/min with the same grinding layer properties as the end face processing wheel.

To analyze the radial wear of the grinding tools along the width of the abrasive layer the grinding wheel surface was measured by a confocal microscope of the type Confovis Duo Vario at three points on the grinding wheel circumference. For each measuring point a height map with two zones is gained. These zones are the contact zone and the reference zone which was not involved in the operation. The radial wear of any point in the contact zone was calculated by the height difference between this point and the height of the reference zone. The cutting edge quality of the end mill cutters was evaluated by measuring the average arithmetic roughness R_a (DIN EN ISO 1302) by a microscope of the type AliconaG5 infinite focus. The four cutting edges of each of the ten end milling cutters produced were analyzed for each grinding tool.

3) Load Optimized Grinding Wheel Design

In the following section a model for the determination of a gradient is derived based on the knowledge of the local related material removal rate (chapter 2.2). A direct mathematical calculation of the related material removal rate is feasible for geometrically simple grinding processes. Fig. 1 presents the results of the simulation of the related material removal rate along the grinding tool width for the previously mentioned parameters.

Figure 1 shows that a variation of the feed rate only means a change of the absolute values of Q'_w . Also a higher cut of depth increases the amount of the values of Q'_w , but does not influence the course of Q'_w over the grinding wheel width. When considering the core diameters an additional change in the course of the curves can be seen. However, the curves are qualitatively comparable. By considering a relative course of Q'_w related to the respective maximum value, a superposition of the curves results, shown in Fig. 1. It is possible to make this adjustment because a higher initial value of Q'_w increases the overall amount of wear, but does not affect its progression across the grinding wheel width. This allows the development of a graded grinding tool which can be used for several investigated applications at the same time if the condition of congruence of the curves is fulfilled. The increased amount of wear at a higher depth of intervention can be counteracted by adapting the feed rate.

To develop a model for wear leveling, the grinding tool must first be divided into a defined number of segments i . Until now, only the production of discontinuous gradients is possible in manufacturing. For this reason, the grinding tool must be subdivided along the grinding wheel width into segments that can be implemented in terms of manufacturing technology. To adjust the load per abrasive grain, it is necessary to know how many abrasive grains are in a certain segment i . This is described by the area-related number of grains $N_{A,i}$. It provides information about the number of abrasive grains per unit area, but not about their shape and size. The area-related number of grains is calculated according to the model of *Friemuth* in equation 2 [14].

$$N_{A,i} = \frac{D_i}{2} \frac{C_i}{\rho \cdot V_{\text{Grain}, i}} = \frac{C_i}{D_i^2} \frac{3}{\pi \cdot \rho} \quad (2)$$

To calculate $N_{A,i}$ of the respective segment i , the grain size D_i , the grain concentration C_i , and the density of diamond has to be considered. The grains are treated simplified as spheres. The first step is to calculate $N_{A,i}$ in the segment of the grinding wheel at which Q'_w has its maximum. There is the highest load per abrasive grain. This segment is defined as the initial segment ($i = 1$). To calculate the initial value, the grain concentration and the grain size must be specified for segment 1, which are summarized in $N_{A,1}$. Thus, the grinding tool specific constant B is calculated according to equation 3:

$$B = \frac{Q'_{w,1}}{N_{A,1}} = \text{const.} \quad (3)$$

The values for B of different grinding wheels are shown in Table 1.

Table 1 Values for the grinding tool specific constant B .

first segment $i = 1$			
C_1	D_1	$N_{A,i}$	B
C80	D46	90.52	0.1895
C100	D46	113.14	0.1516
C100	D54	82.10	0.2089
C125	D54	102.63	0.1671

Together with equations 2 and 3, B is used to calculate the necessary grain concentration, or grain size, for all further segments of the grinding tool ($i > 1$) to keep the local related material removal rate per abrasive grain constant:

$$C_i = Q'_{w,i} \cdot D_i^2 \cdot \frac{\rho \cdot \pi}{3 \cdot B} \quad (4)$$

In Fig. 2, the gradient calculated with the model is shown for a grain size and a grain concentration gradient. A grain size of D46 and a grain concentration of C100 were set as initial values to calculate B . As values for Q'_w the previously considered simulation results for a core diameter of $k = 0.7$ and the process parameters described in chapter 2.2 were used.

Fig. 2 shows three possibilities to develop a gradient. First a grain concentration gradient can be applied. The concentration gradient can be adjusted in any small step by the mixing ratio of grain and bond material, restricted by limitations of manufacture. Secondly, a gradient can be applied by varying the

grain size. A reduction of the grain size at a constant concentration increases the area-related number of grains. The approach is limited by commercially available grain and mesh sizes. Result is a gradient with a scatter band (see Fig. 2). The third possibility is a hybrid gradient as a combination of grain size and concentration variation. This gradient exhibits the smallest global differences between grain size and grain concentration along the grinding tool width. Reduced global differences provide a more uniform grinding behavior. For all three types of gradients, the segment width that can be produced is decisive. The smallest possible segment width that could be practically implemented was assumed as 1 mm. Based on the results from Fig. 2 three gradients were determined, which were manufactured by the grinding tool manufacturer Dr. Müller Diamantmetall AG. These gradients are shown in Table 2.

Table 2 Gradients of the used grinding wheels. Grain concentration and grain size are specified according to FEPA standard.

#	grinding wheel width b in mm									
	0 - 1	1 - 2	2 - 3	3 - 4	4 - 5	5 - 6	6 - 7	7 - 8	8 - 9	9 - 10
1	C125	C110	C110	C100	C100	C90	C90	C80	C80	C80
	←—————				D54 = const.		—————→			
2	C100	C125	C125	C110	C110	C100	C100	C90	C90	C90
	D46	←—————			D54 = const.		—————→			
3	C80	C100	C100	C90	C90	C80	C80	C70	C70	C70
	D46	←—————			D54 = const.		—————→			

These grinding tools are evaluated in the following chapters regarding their wear behavior and the quality of the milling tools. The limitation of the minimum manufacturable segment width leads to differences between the targeted number of grains and the number of grains in the segments of the produced grinding tool.

Fig. 3 shows that the differences between the simulated concentration gradient and the produced gradient are very high at the transitions between the segments.

4) Influence Of The Gradient On The Wear Behavior

The results from the wear investigation are presented in the following section. These were carried out as described in chapter 2 with the two not graded and the three graded grinding tools according to the design from Chapter 3. Fig. 4 displays the results of the calculated radial wear over the grinding wheel width.

Two observations can be drawn from the consideration of the not graded grinding wheels. On the one hand, the course of the radial wear over the grinding layer width corresponds qualitatively to the simulated course of the associated related material removal rate. However, it can be observed that the negative course in the range between 1 and 2.5 mm of the grinding layer width is higher than the corresponding course of the related material removal rate. This can be explained by not considering the influence of thermal load, which is difficult to simulate for deep groove grinding so far, or further geometrical influencing factors. Furthermore, the geometric contact length also varies along the grinding wheel width. This influences h_{cu} , which has an influence on the forces acting on the abrasive grains. As a result, radial wear increases disproportionately to Q'_w . On the other hand, it shows that a higher grain concentration reduces wear for the application considered. That effect refers to a more uniform load distribution at higher grain concentrations, decreasing the total load per grain by a reduced single grain chip thickness. However, an increase in grain concentration is limited by a bond system-dependent percolation threshold given through the reduction of grain retention by the bond due to a high abrasive grain volume fraction [15]. From these observations, it is shown that by adjusting the grain concentration, wear is influenced. Evidence that increasing the grain concentration reduces radial wear is illustrated in Figure 5.

The diagram on the right side of figure 4 represents the radial wear curves of the three graded grinding tools. The wear behavior of these tools differs from that of the not graded tools, which exhibit geometry-dependent wear behavior. The graded grinding wheel #1 with the grain concentration gradient shows a low radial wear in the first segment (0 to 1 mm), followed by a clear increase in the following two segments (1 to 3 mm). The cause is the large difference in concentration between the two sections (C125 to C110). At these points, the wear is increased in the range up to 2.5 mm grinding wheel width. In these segments, the load on the grinding tool is highest and the relative difference of the concentration is most pronounced. Therefore, the influence of this effect is reduced with decreasing l_g and Q'_w . Since no repeat measurements are possible due to the time-consuming experimental effort, a scattering of the measurement results cannot be excluded. It can be stated that for a smoother transition smaller concentration steps must be applied. Considering this, the hybrid graded wheels #2 and #3 (Table 2) were designed. In these, a step in the grain concentration also occurs between segments 1 and 2, but this is countered by the adjustment of the grain size.

For the grain concentration gradient, the difference in grain concentration is at C45, while for the hybrid gradients, the differences are at C35, and C30, respectively. This corresponds to a 22 to 33 percent reduction in grain concentration differences. Due to the influence of the grain concentration on the grinding forces, a reduction of the force differences over the grinding wheel width compared to the concentration gradient can also be expected. When analyzing their curves in Fig. 3 both show a similar behavior. Beside the sections from 0 to 2 mm of the grinding wheel width with the highest radial wear, the radial wear behavior in the remaining sections is more uniform. This area demonstrates the necessity of adding a factor to the model created in Chapter 3 (equation 4) to consider thermal loads for optimizing the grinding tool. In particular, the thermal load often defines the process limits in deep groove grinding

and can thus be associated with the strong increase in wear in the area of a high depth of cut [16]. A purely experimental approach can iteratively lower the wear in these areas by increasing the grain concentration, as shown in the results of the ungraded grinding wheels, too. Apart from this, it also shows that a reduction of the wear difference is possible by adjusting the area-related number of grains to the local related material removal rate according to formula 4. Fig. 6 shows the maximum difference in radial wear for all grinding tools used. It gives an overview of the extent to which the grinding tools manufactured according to the model introduced in chapter 3 were able to level out the wear over the grinding layer width.

By a comparison with the constant grinding wheel (C125, D54) with a maximum height difference of 29.99 μm the graded wheel (#3) has a height difference of 14.41 μm and thereout a wear difference reduction of about 51.95 %. The grinding wheel #2 enables a reduction of the difference of 46.44 % in comparison to the reference grinding wheel. Compared to the hybrid gradients the concentration gradient (wheel #1) provides just a small levelling of about 17.14 %. This shows that equation 4 is a potential approach to derive gradients regarding the number of grains to level the wear behavior over the grinding tool width according to the application. However, it also shows that there is still further potential for optimization since further repeat tests are necessary and other influencing variables, such as thermal load, must also be taken into account. In order to analyze the influence of the gradients on the grinding layer surface topography images are taken after operation.

Fig. 7 shows surface segments of the grinding tools after operation. On the one hand, the greater wear difference can be seen for the non-graded grinding tools. On the other hand, it can be seen that in the wear-intensive areas (segments from 0 to 2.5 mm), the surfaces appears more fragmented than in the areas with lower wear. This is an indication of the change in wear mechanisms between the zones described. The observation of the graded grinding wheels, on the other hand, shows that this difference is much less pronounced. For grinding wheel #1, the transition zone from the edge zone with the high concentration C125 to the concentration C110 can be observed. Grinding wheel #3, on the other hand, has a zone of 2.5 to 7.5 mm in the central area of the grinding layer, in which the wear is low, and an optically cutting-friendly topography can be seen.

5) Analyzes Of The Cutting Edge Quality

To be suitable for industrial use, the graded grinding tools must prove that they do not reduce the workpiece quality, such as the chipping, the rounding of the cutting edge, or the roughness of the rake face or flank, of the carbide cutters due to the altered abrasive layer properties. As described in chapter 2, for the evaluation of the deep groove grinding, especially the chipping of the cutting edge is used to describe the process quality. [10]. Fig. 8 shows the results in the form of the arithmetic mean roughness R_a .

Figure 8 shows that lower radial wear in the area of the grinding tool edge can reduce chipping while otherwise maintaining the same abrasive layer properties. This can be observed when comparing the

constant grinding wheel with C125 to the graded grinding wheel #1. This can be the result of more uniform engagement conditions between the grinding wheel and the workpiece as well as less breakouts in the grinding layer. This can also be seen when looking at the topography images in Fig 7, in which the ungraded grinding wheel (C125) shows more breakouts in the range of 0 to 1 mm grinding wheel width. Therefore, higher grinding tool stability at the edge due to the gradient can improve the application behavior [17]. Furthermore, as expected, reduced grain size reduces the roughness. Smaller grain protrusions result in a reduced roughness depth on the workpiece surface. However, a reduction in the grain concentration (grinding wheel #3 against #4) increases as expected the chipping again, as this increases the single grain chip thickness [12, 18]. The effect of the grain size outweighs the influence of the grain concentration with a constant area-related grain number. This can be seen from the comparison of grinding wheels #1 and #2. Grinding wheel #2 has a lower concentration (C100) than grinding wheel #1 (C125) which should increase the roughness. Both the smaller grains of #2 (D46) against #1 lead to decreased roughness instead of the concentration effect. It can be deduced, that a hybrid gradient with a smaller grain size in the grinding wheel edge area leads to decreased cutting edge roughness, despite the lower grain concentration.

6) Conclusions

The results show that the wear is influenced by the area-related number of grains. It was shown that a model can be derived to develop a gradient which reduces the wear depending on the local related material removal rate. From the grinding studies, it has been shown that the hybrid gradient levels the wear better than a pure concentration gradient. This is due to a smaller difference in the abrasive properties of the hybrid gradient compared to the grain concentration gradient. Likewise, it has been shown that the hybrid gradients reduce the cutting edge roughness for the considered application. From this it can be deduced that the model can be used to design a uniformly wearing grinding tool for a pre-defined cutter geometry. The investigations also show that it is necessary to consider other influencing variables, such as thermal loads. Especially in the area of the highest occurring radial wear an optimization potential was shown. This potential can be achieved by extending the introduced model through knowledge of other factors influencing wear along the grinding wheel width or by an iterative approximation. Furthermore, it is also necessary to map the grain size and grain concentration gradient in the grinding tools in smoother steps. It is therefore necessary to extend the model and to adapt the manufacturing process in order to achieve leveled wear behavior.

Abbreviations

a_e	Depth of cut in mm
b	Grinding wheel width in mm
B	Related material removal rate per abrasive in $\text{mm}^3/\text{mm s}$
C	Concentration of abrasive 4.4 g/cm^3
D	Abrasive grain size in μm
d_k	Tool core diameter in mm
d_s	Tool diameter in mm
i	Number of grinding wheel segment (-)
k	Tool core diameter factor (-)
N_A	Area related number of grains (-)
l_g	Geometric contact length in mm
Q'_w	Related material removal rate in $\text{mm}^3/\text{mm s}$
Δr	Radial wear in μm
R_a	Average arithmetic roughness in μm
v_c	Cutting speed in m/s
v_f	Feed rate in mm/min
V	Abrasive grain volume in μm^3
z	Number of teeth (-)
δ	Helix angle in $^\circ$
ρ	Density in g/cm^3

Declarations

Funding

The investigations were funded by the Federal Ministry for Economic Affairs and Energy (BMWi) as part of the Central Innovation Programm for small and medium-sized enterprises (SMEs) (ZIM) within the project "Graded grinding wheels for deep grinding of cemented carbide end mills" (ZF4070519TV9) based on a resolution of the German Bundestag.

Conflicts of interest/Competing interests

The Authors declare that they have no conflict of interest.

Availability of data and material

- Not applicable -

Code availability

- Not applicable -

Authors' contributions

Prof. Dr.-Ing. Berend Denkena was responsible for funding acquisition and project administration and reviewed and edited the article together with Dr.-Ing. B. Bergmann in the writing process.

Dr.-Ing. Benjamin Bergmann supervised the project.

Daniel Raffalt conducted the experiments, analyzed the data and wrote the manuscript.

Acknowledgments

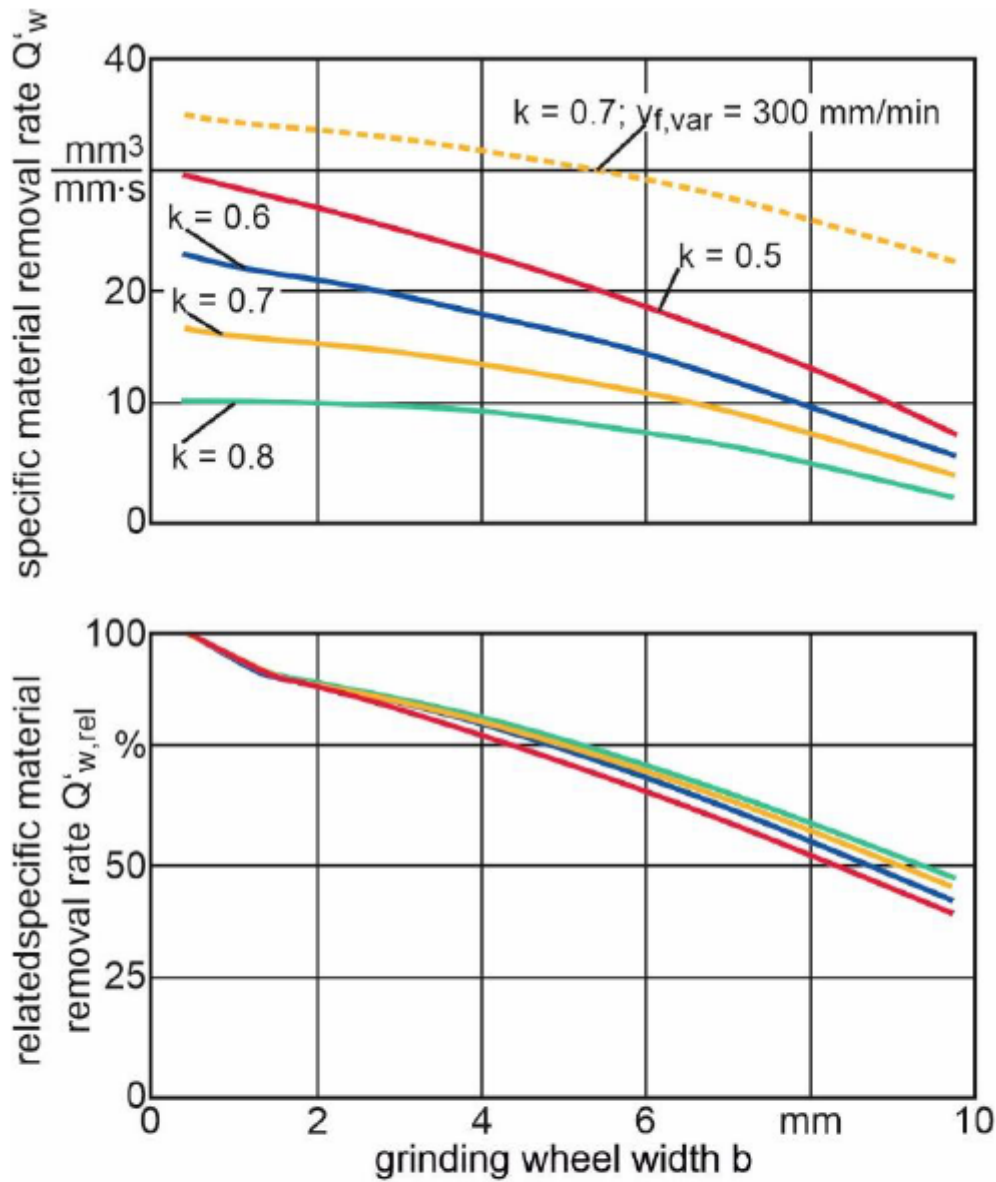
The authors thank the Federal Ministry for Economic Affairs and Energy (BMWi) for the support and the project partner Dr. Müller Diamantmetall AG for the constructive and close cooperation.

References

- [1] Malkin S., Guo, C. (2008): Grinding technology: theory and application of machining with abrasives. 2nd Edition, Industrial Press Inc
- [2] Mayr J., Barbist, R. (2014): Untersuchung und Bewertung der Schleifbarkeit von Hartmetall. Der Stahlformenbauer 31 4: 74 - 79
- [3] Uhlmann E., Hübert C. (2011): Tool grinding of end mill cutting tools made from high performance ceramics and cemented carbides. In: CIRP Annals - Manufacturing Technology, Vol. 60: 359 – 362, Issue 1
- [4] Heymann T. (2012): Gezielte Nut- und Schneidkantenpräparation von Vollhartmetall - Zerspanwerkzeugen durch Polierschleifen. In: Spanende Fertigung / Prozesse – Innovation – Werkstoffe. 6. Ausgabe (2012), Vulkan-Verlag Essen: 104-110
- [5] Schröer N. (2018): Spannutschleifen von Hartmetall-Schaftwerkzeugen mit gradierten Schleifscheiben. Dr.-Ing. Dissertation, Technische Universität Berlin
- [6] Lierse T. (1998): Mechanische und thermische Wirkungen beim Schleifen keramischer Werkstoffe. Dissertation, Hannover

- [7] Demir H., Gullu A. (2001): The effect of parameters in the grinding. In: Journal of Engineering Sciences, vol. 7: 189-198.
- [8] Ohmori H.; Kasai T. (1997): Development of metal-resin bonded diamond wheel for ELID-lap grinding and its grinding performance. In: ICPE '97, Taipei, Taiwan: 177-181
- [9] Uhlmann E., Schröder N. (2016): Werkzeugschleifen mit Hybridschleifscheiben: Vergleich unterschiedlicher Schleifscheibenbindungsspezifikationen beim Nutentiefschliff von Hartmetall. In: wt Werkstattstechnik online 106: 181–186
- [10] Dröder K.; Karpuschewski B.; Uhlmann E. (2020): A comparative analysis of ceramic and cemented carbide end mills. Production Engineering volume 14: 355-364
- [11] Biermann D., Schumann S., Kansteiner M. (2012): Umfassende Betrachtung der mechanischen Belastungen im Schleifprozess. In: Forum Schneidwerkzeug- und Schleiftechnik: 72 - 83, No. 4/2012
- [12] Bifano T. G., Dow T. A., Scattergood R. O. (1991): Ductile-Regime Grinding. A New Technology for Machining Brittle Materials. In: Journal of Engineering for Industry. 113. Jg.: 184-189, No. 2
- [13] Denkena B., Böß V. (2009): Technological NC simulation for grinding and cutting processes using CutS. In: Proceedings of the 12th CIRP conference on modelling of machining operations
- [14] Friemuth T. (2002): Herstellung spanender Werkzeuge. Habilitation thesis, Universität Hannover
- [15] Denkena B., Grove T., Göttching T., Dzierzawa P., Kempf F. (2017): Methods of analysis for a deeper understanding of the grinding process. In: Proceedings of the 20th International Symposium on Advances in Abrasive Technology: 945–951
- [16] Jin T.; Stephenson D. J. (2006): Heat flux distributions and convective heat transfer in deep grinding. International Journal of Machine Tools & Manufacture 46, 14: 1862-1868
- [17] Sroka F. (2005): Konditionieren von Diamantschleifscheiben. Dr.-Ing. Dissertation, Technische Universität Berlin
- [18] Fritsch A. (1997): Schleifen von Cermets. Dr.-Ing. Dissertation, Leibniz Universität Hannover

Figures



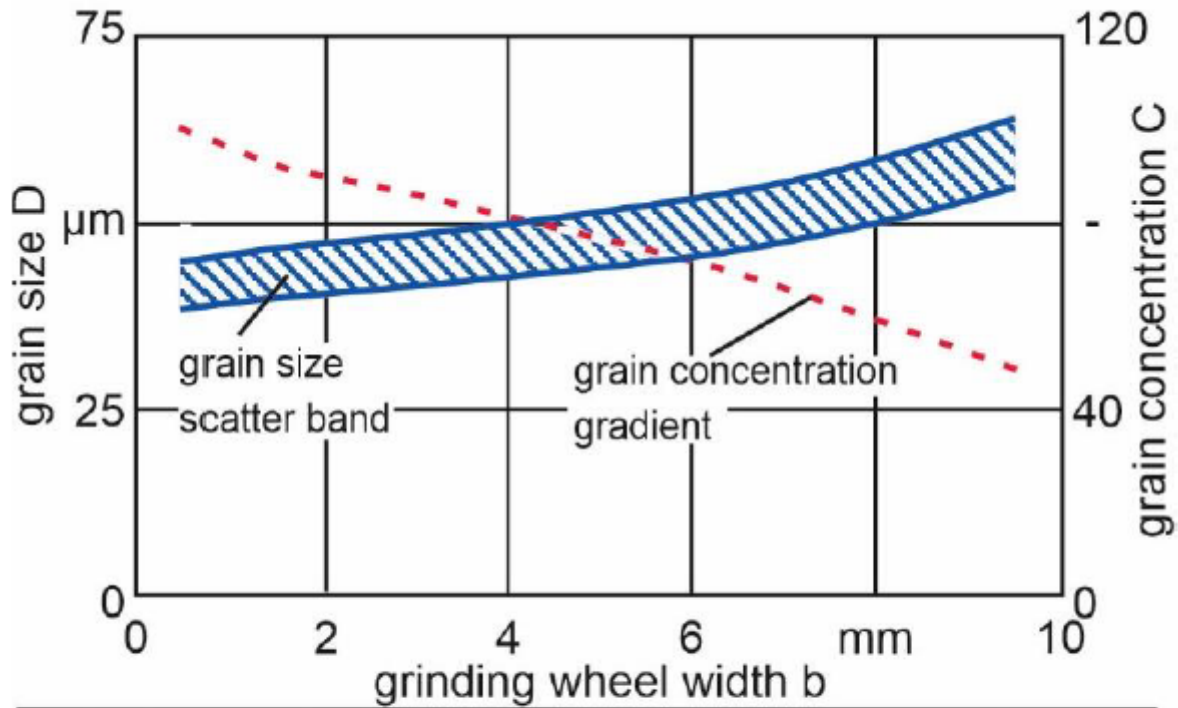
end mill specifications	process variables	grinding wheel
$z = 4$	$v_f = 150 \text{ mm/min}$	1A1-100-10-6-20
$\delta = 30^\circ$	$v_{f,var} = 300 \text{ mm/min}$	
$d_s = 16 \text{ mm}$		
$k = 0.8, 0.7, 0.6, 0.5$		

Rf/103985 © IFW

Figure 1

Simulated related material removal rate for flute grinding of end mill cutters and the calculated relative curves.

requirement: constant load per abrasive grain



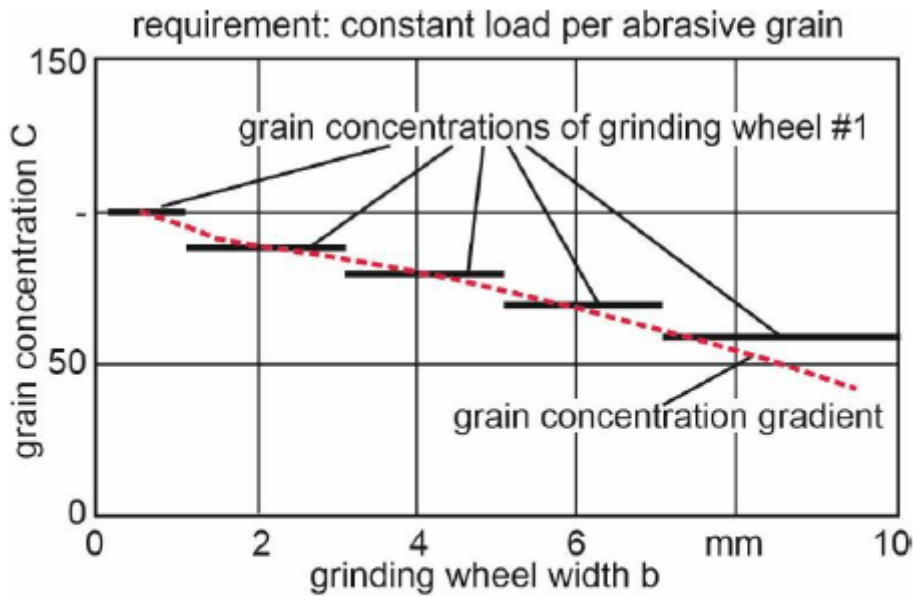
end mill	grinding wheel	process parameters
$z = 4$	Bond material: hybrid	$v_f = 150 \text{ mm/min}$
$\delta = 30^\circ$	Abrasive: diamond	$v_c = 18 \text{ m/s}$
$d_s = 16 \text{ mm}$		
$k = 0.7$		



Rf/103997 ©IFW

Figure 2

Possible grain size and grain concentration gradient.

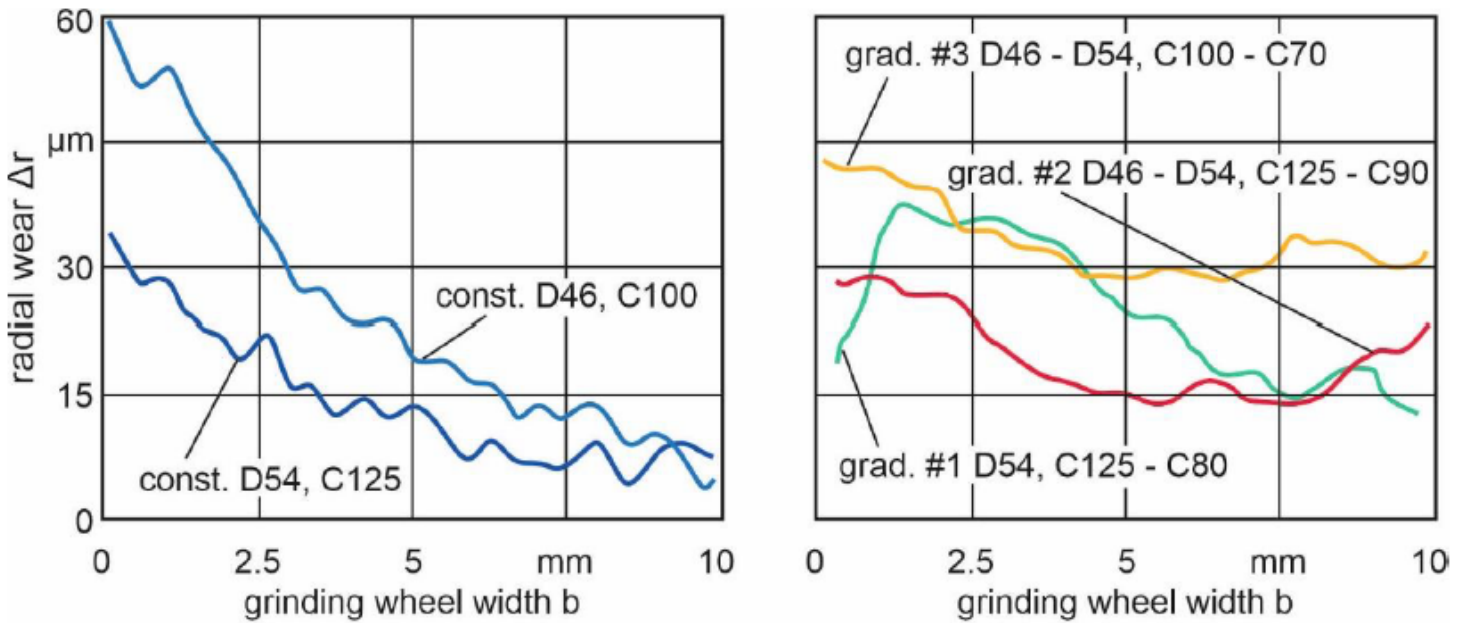


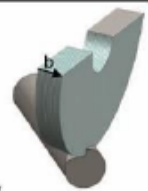
end mill	process parameters	grinding wheel	
$z = 4$	$v_f = 150 \text{ mm/min}$	Bond material: hybrid	
$\delta = 30^\circ$	$v_c = 18 \text{ m/s}$	Abrasive: diamond	
$d_s = 16 \text{ mm}$			
$k = 0.7$			

Rf/103996 © IFW

Figure 3

Comparison between the manufactured and the simulated grain concentration curve.

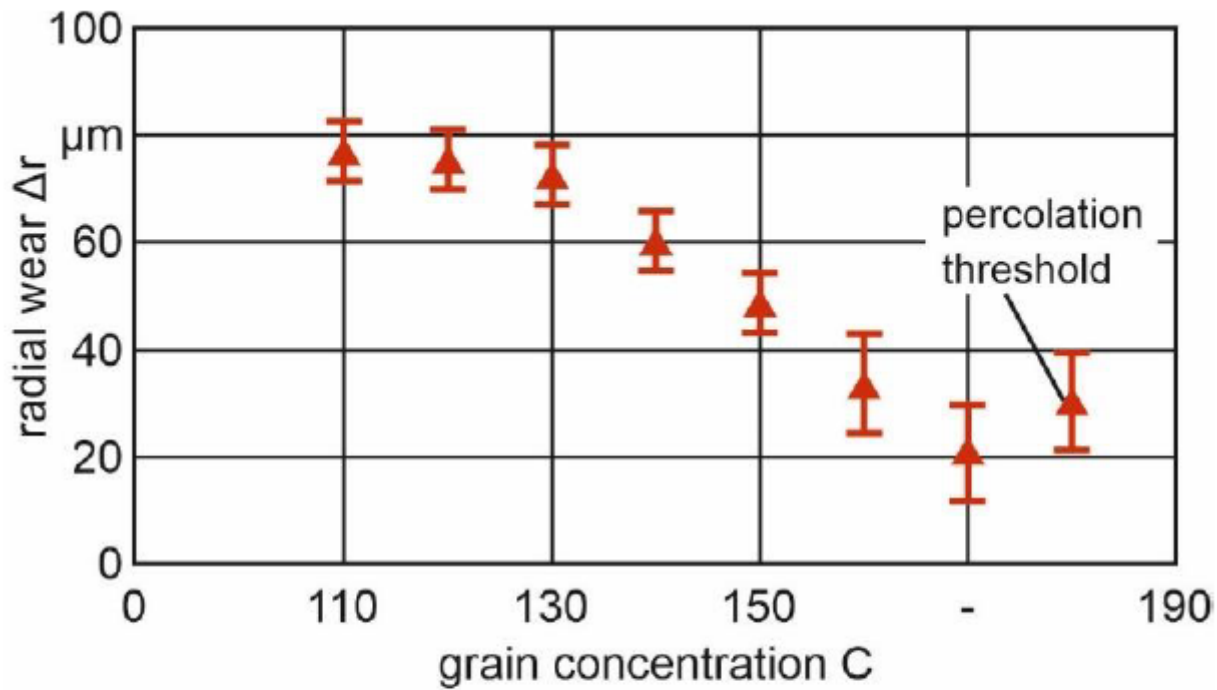


end mill specifications	process parameters	grinding wheel	
$z = 4$	$v_f = 180 \text{ mm/min}$	Bond material: hybrid	
$\delta = 30^\circ$	$v_c = 18 \text{ m/s}$	Abrasive: diamond	
$d_s = 16 \text{ mm}$			
$k = 0.7$			

Rf/109150 © IFW

Figure 4

Radial wear over the grinding wheel width.



process parameters

depth of cut $a_e = 6.0$ mm
width of cut $b_e = 4.0$ mm
cutting length $l_s = 100$ mm
feed rate $v_f = 100$ mm/min
cutting speed $v_c = 25$ m/s

materials

cemented carbide:
EMT 210 (10 % Co, 0.8 μm)
grinding wheel:
1A1-100-10-6-20-D54

Rf/104023 © IFW

Figure 5

Influence of grain concentration on radial wear.

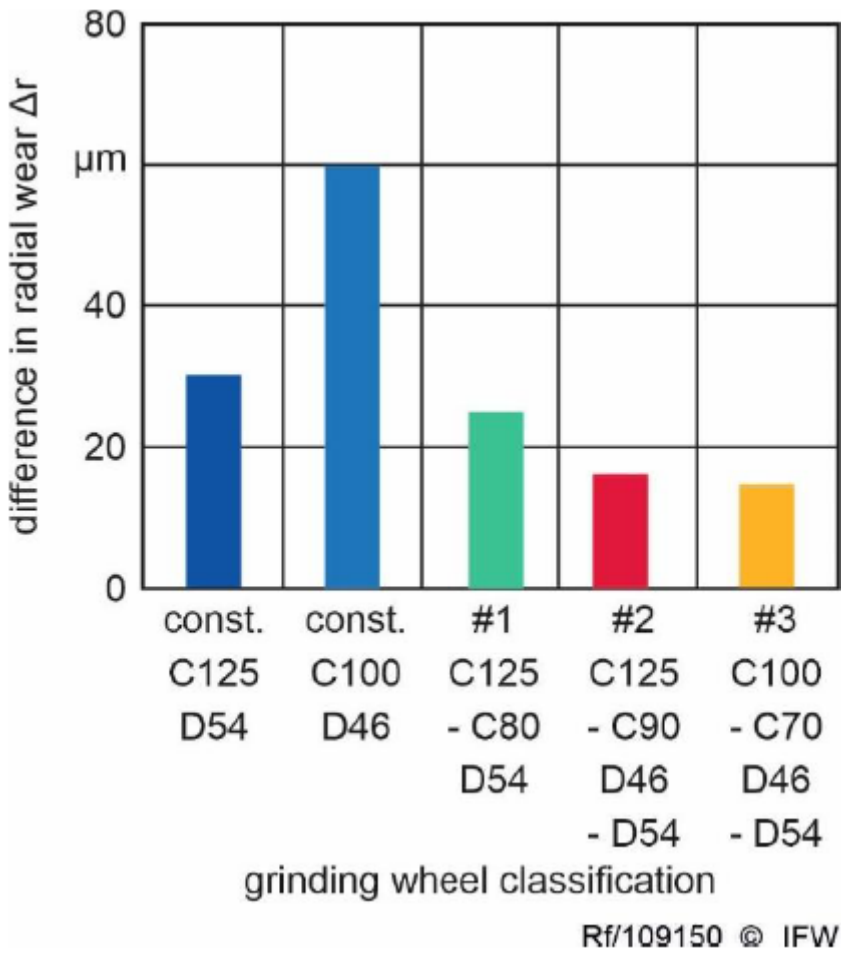


Figure 6

Absolute radial wear differences for the investigated grinding wheels.

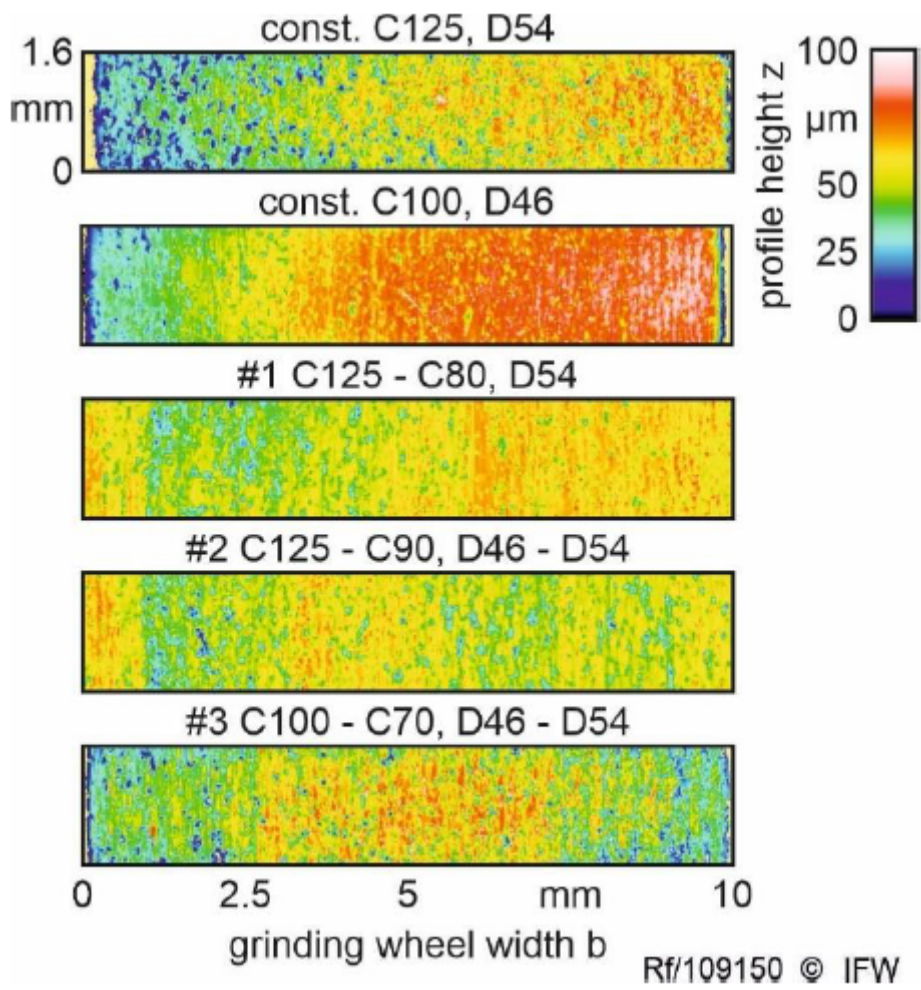


Figure 7

Surface segments of the grinding tools after operation.

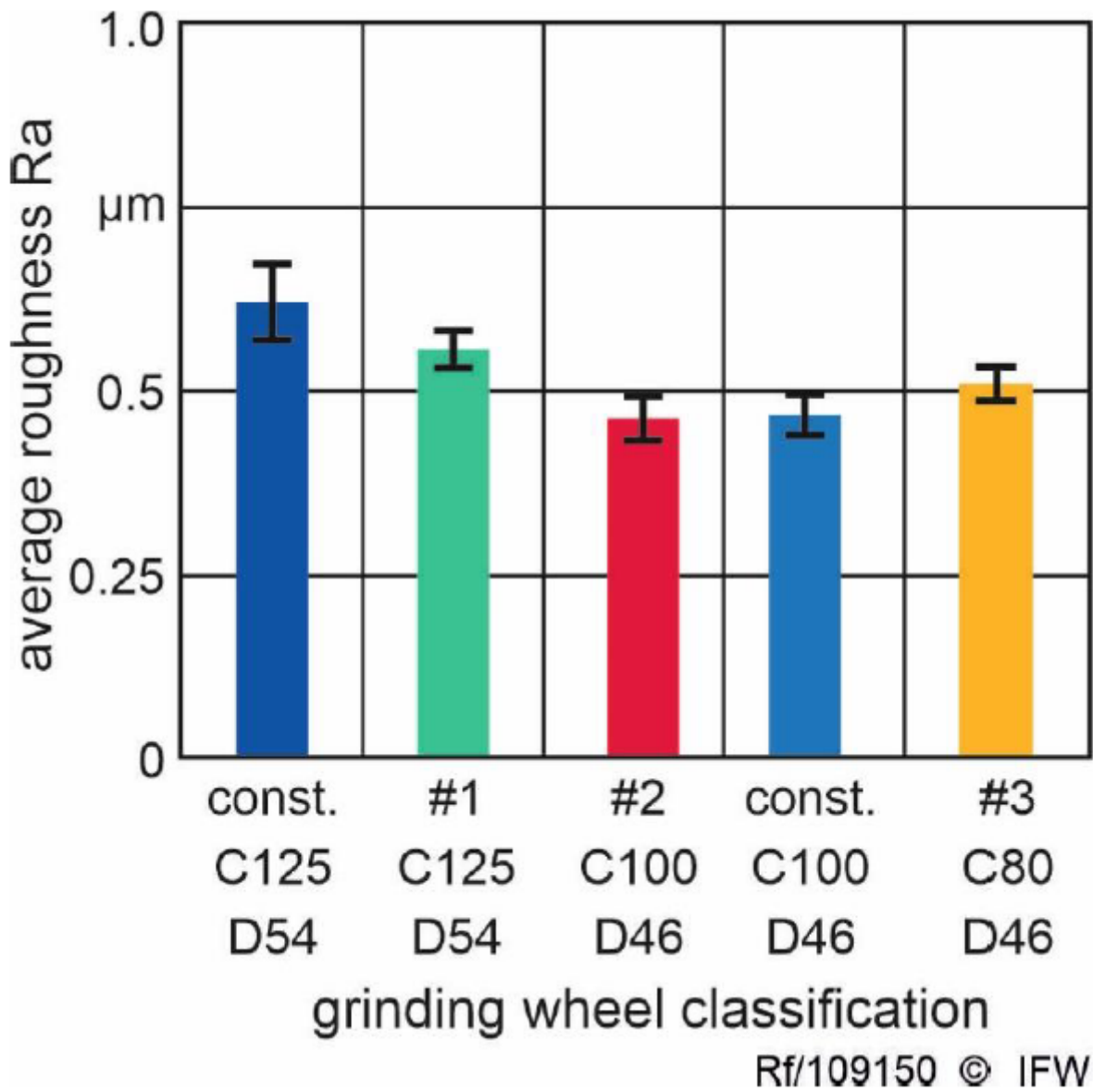


Figure 8

Average roughness of the end mill cutting edges after grinding for the grinding layer parameters concentration and grain size at the grinding wheel edges.